Dissociation kinetics of hydrogen-passivated (111) Si-SiO_2 interface defects

K. L. Brower
Sandia National Laboratory, P.O. Box 5800, Albuquerque, New Mexico 87185-5800
(Received 23 March 1990)

This paper is concerned with the chemical kinetics of the transformation of hydrogen-passivated interface defects (HP_b centers) into paramagnetic P_b centers ($\cdot Si \equiv Si_3$) at the (111) Si-SiO_2 interface under vacuum thermal annealing. Float-zone (111) silicon substrates were oxidized in dry oxygen at 750 °C to a thickness of 500 Å, passivated with H_2 (D_2) at 300 °C for 3 h (4 h), and then vacuum thermal annealed at temperatures ranging from 500 to 595 °C. The results of this analysis indicate that the kinetic process is described by a first-order rate equation $d[HP_b]/dt = -k_d[HP_b]$ where $k_d = k_{d0}\exp(-E_d/kT)$. An activation energy of 2.56 ± 0.06 eV with a preexponential factor k_{d0} of approximately 1.2×10^{12} sec^{-1} was obtained. The reaction rate is reduced if the samples are passivated with deuterium instead of hydrogen. These results suggest that the chemical process is due to the thermal decomposition of the HP_b center into P_b centers and atomic hydrogen. Although the activation energy for the diffusion of interstitial oxygen in silicon is also 2.56 eV, a rate-limiting step involving this mechanism is inconsistent with the hydrogen isotope effect as well as other considerations. Comparison of the activation energies for the H_2 passivation of the P_b center and dissociation of the HP_b center are shown to be chemically and energetically equivalent to the dissociation of the H_2 molecule as originally indicated by Myers and Richards. Thus, the reverse passivation reaction, $H + HP_b \rightarrow P_b + H_2$, and the reverse dissociation reaction, $H + P_b \rightarrow HP_b$, are exothermic reactions that proceed with very little thermal activation in the presence of atomic hydrogen.

I. INTRODUCTION

An insulating layer (≤ 1 μm) of SiO_2 atomically bonded to semiconducting silicon can be made simply by heating silicon in oxygen. Ordinarily, the crystalline silicon atoms at the Si-SiO_2 interface bond to oxygen atoms of the SiO_2; nevertheless, up to approximately 0.5% of the crystalline interfacial silicon atoms are not bonded to oxygen atoms and give rise to a specific dangling bond type of defect, $\cdot Si \equiv Si_3$, called the P_b center. In the neutral charge state this interface defect is observable with electron paramagnetic resonance (EPR).[1-3] The paramagnetism of this defect arises from an unpaired electron localized in a $sp^3_{[111]}$-like hybrid orbital localized on the defect silicon atom.[4,5]

These defects are believed to be the dominant interfacial charge traps that make this insulator-semiconductor (IS) system less than ideal in device applications.[6,7] In order to minimize the effects of charge trapping at such defects, the defects are exposed to hydrogen, the idea being that the hydrogen will chemically bind to and passivate these defects. The effects of hydrogen on interface states have been observed previously by electrical measurements.[8-11] The electrical measurements require a conducting gate on top of the oxide forming a metal-insulator-semiconductor (MIS) structure. For the case of Al-SiO_2-Si device structures, passivation of Si-SiO_2 interface states is achieved simply by heating the device structure to 200 °C independent of the gas ambient.[9] Do Thanh and Bauk[8] have suggested that in this case passivation occurs as a result of the generation of atomic hydrogen at the Al-SiO_2 interface; this source of hydrogen is attributed to prior contamination during device processing. In this case, a hydrogen atom, or a proton, which might behave like a polaron, diffuses to the P_b center to form a HP_b center. (A model illustrating the atomic structure of the passivated P_b center is illustrated in Sec. IV B in Fig. 10.) Reed and Plummer[9] have recently characterized the kinetics of this process using capacitance-voltage (C-V) measurements. Since the work function of polysilicon essentially matches that of the silicon substrate, polysilicon gates have for the most part supplanted aluminum as a gate material in commercial applications. Fishbein, Watt, and Plummer[10] attempted to determine the kinetics of passivation using molecular hydrogen. In their experiments passivation occurred by a mechanism in which H_2 entered the oxide primarily at exposed SiO_2 edges. Since it was necessary for H_2 to diffuse laterally distances up to 50 μm, the rate-limiting step observed in their C-V measurements was the diffusion of H_2 in the oxide rather than the passivation of the interface states.[10]

Recently, we[12] determined from EPR measurements the chemical kinetics for the passivation of a specific interface defect, namely the P_b center, using molecular hydrogen. The simplicity in sample preparation and structure needed for EPR measurements avoids many of the complications inherent in preparing device structures for electrical measurements. In our experiments (111) silicon substrates were oxidized to a thickness of 500 Å and exposed to H_2 under conditions for which the time, temperature, and H_2 pressure were known. All processing steps

were accomplished *in situ* within a quartz tube to minimize any effects due to extraneous hydrogen-related contamination. We determined that the rate of passivation was given by the expression

$$\frac{d[P_b]}{dt} = -k_f^{(2)}[H_2][P_b] , \quad (1)$$

where $k_f^{(2)}$ obeys the Arrhenius equation

$$k_f^{(2)} = k_{f0}^{(2)} \exp(-E_f/kT) . \quad (2)$$

The volume concentration of H_2 at the interface and within the thermal oxide was assumed to be the same as the physical solubility of molecular hydrogen in bulk vitreous silica[12] as determined theoretically by Shackelford, Studt, and Fulrath[13] and empirically by Shelby.[14] Since the equilibrium time for the hydrogen concentration within the thermal oxide was very short (<1 sec) compared to the times required for measurable passivation (>100 min), the rate-limiting step was the passivation reaction itself.

From the nature of the kinetic equation [Eq. (1)] and the magnitude of the preexponential constant in Eq. (2), we suggested a physicochemical process by which P_b centers are passivated. According to this model, H_2 is physically absorbed into the SiO_2 and diffuses as H_2 among the accessible interstices of the SiO_2 network including the reaction site at the P_b center. During times that a H_2 molecule is adjacent to the P_b center, there is a finite probability that it will react with the P_b center according to the chemical reaction

$$H_2 + P_b \rightarrow HP_b + H , \quad (3)$$

resulting in the passivation of the P_b center and the formation of a diamagnetic HP_b center.

Now, another problem arises and is the focus of study in this paper. Although thermal annealing in H_2 results in the disappearance of the P_b resonance, subsequent vacuum thermal annealing above 500 °C causes the P_b centers to reappear. The purpose of this paper is to determine the physiochemical process by which P_b centers reappear upon subsequent vacuum thermal annealing. In this study we are able to show that the P_b centers reappear as a result of thermally activated dissociation of HP_b centers. Another model involving the reduction of HP_b centers by mobil interstitial oxygen from within the silicon is shown to be inconsistent with our experimental results.

From this work and one other observation, namely that the sequence of the passivation and dissociation reactions are equivalent to the dissociation of the H_2 molecule, emerges a unified model for the hydrogen chemical kinetics of P_b centers. There is reason to believe that the activation energies for the passivation and dissociation reactions are equal or only slightly greater than the energy difference between the respective initial and final constituents.[15,16] Consequently, the reverse passivation and dissociation reactions are predicted to proceed essentially spontaneously in the presence of atomic hydrogen and are expected to be important in a radiation environment.

The details of our sample preparation and EPR measurements are presented in Sec. II. The results of our EPR measurements are represented phenomenologically in terms of first-order kinetics in Sec. III. Also included in this section are the results of our studies using different hydrogen isotopes. In Sec. IV, two physicochemical models designed to account for the reappearance of the P_b center upon vacuum thermal annealing after H_2 passivation are examined in terms of our experimental results. In Sec. V the energetics of the passivation and dissociation processes, which are sequentially equivalent to the dissociation of the hydrogen molecule, are analyzed and the nature of the energy barriers for the various reactions is discussed. Our conclusions derived from this study are presented in Sec. VI.

II. EXPERIMENTAL TECHNIQUES

A. (001) versus (111) Si-SiO_2 interface

Electron paramagnetic resonance measurements of P_b-type defects on the (111) rather than the (001) Si-SiO_2 interface are preferred for two reasons. First, the signal-to-noise ratio is greater in the case of the (111) interface because of its greater interface state density. Second, the (111) Si-SiO_2 interface has only one type of paramagnetic defect, namely the P_b center, whereas two distinct paramagnetic defects, namely the P_{b0} and P_{b1} centers, are associated with the (001) Si-SiO_2 interface. These two defects give rise to only two partially overlapping resonances providing the applied magnetic field is perpendicular to the (001) interface.[17] These complications make it very difficult to measure the intensity of the individual defect spectra associated with the (001) interface. Thus, this kinetic study is limited to the (111) interface. At this time our understanding of the structure of the P_b defect associated with the (111) Si-SiO_2 is far more advanced than our understanding of the P_{b0} and P_{b1} centers associated with the (001) interface.[5] Although the (111) interface is ideal in many respects for scientific studies, the (001) interface is the one employed in device structures because of its lower density of interface states, nature of the silicon faceting under etching, slightly different surface potential, etc.

B. Sample treatment

The details of our method of sample preparation and measurement have been discussed previously.[12] In this study (111) silicon substrates are thermally oxidized at 750 °C in 760 Torr of dry oxygen for 31 h;[18] this yields an oxide approximately 500 Å thick with approximately 3×10^{12} P_b centers/cm^2. After the samples have cooled to room temperature in vacuum, they are reheated *in situ* and annealed in H_2 (D_2) at 300 °C and 760 Torr for 3 h (4 h); after this treatment, no P_b resonance can be detected in these samples. Finally, after the samples have again cooled to room temperature, the samples are annealed *in situ* in vacuum (approximately 5×10^{-5} Torr) for a given

time and temperature. This vacuum anneal results in a partial recovery of the P_b signal. Only after this final vacuum anneal are the vacuum-pressure seals broken and the samples removed for EPR measurements. The P_b centers are stable at room temperature with the oxide exposed to air.[12] This approach allows us to determine the kinetic parameters that characterize the recovery in the P_b signal.

C. Oxidation-annealing system

The system used for oxidation, hydrogen, and vacuum annealing consists of a 61-cm-long tubular furnace with a 5.1-cm open bore. A 33-mm-diam, 127-cm-long quartz tube is placed on the axis of the furnace. This tube can be evacuated with a turbomolecular pump or back filled with a gas. The sample holder, shown in Fig. 1, containing our silicon samples to be processed is slipped into this quartz tube. For purposes of quick heating or quenching, the furnace can be repositioned along the length of this sample tube. In the region of the sample holder, a ceramic aluminum oxide tube 65 cm long with a 41 mm outside diameter is slipped over the outside of the quartz sample tube. This aluminum oxide tube moderates the thermal radiation from the bare heating coils of the furnace and acts as a blackbody, cylindrical-cavity radiator.

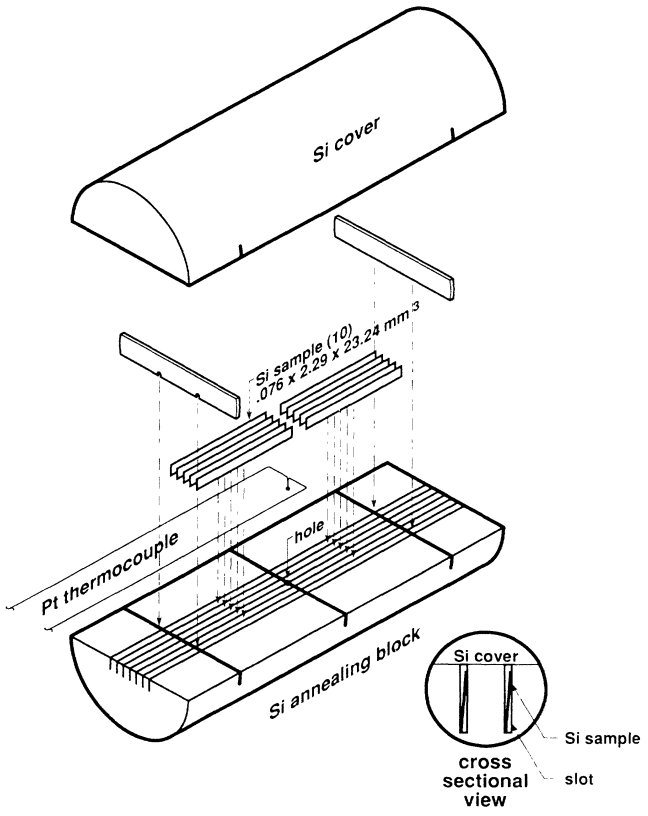

FIG. 1. Schematic of the sample holder in which the silicon samples were thermally oxidized, passivated in H_2, and vacuum thermal annealed. The temperature of the silicon holder is measured with the Pt thermocouple.

The sample holder in which the silicon substrates are oxidized, annealed in hydrogen, and subsequently annealed in vacuum is shown in Fig. 1. This sample holder is made of silicon and acquires an oxidized surface. We chose silicon because it is a very clean material. Oxidation of the silicon is necessary in order to prevent the reduction of the Pt thermocouple to a platinum silicide. The individual silicon samples are placed in the slots as illustrated. Thus, each silicon sample is contained within a thermal radiation cavity.

D. Temperature considerations

As indicated in Fig. 1, the temperature of the sample holder is measured using a Pt thermocouple (type *S*). The first question is how does this temperature relate to the sample temperature, especially in a vacuum environment? Since each sample is contained within a cavity (Fig. 1), each sample necessarily comes to the same temperature as the silicon holder by virtue of energy exchange due to thermal radiation. At 773 K the rate of temperature change for a one-degree-Kelvin temperature difference between sample and holder is approximately 0.9 K/sec; thus, thermal radiation quickly drives these thin, low-mass samples into thermal equilibrium with the silicon sample holder. The second question is since the sample holder in Fig. 1 is heated in vacuum by only thermal radiation, what is the maximum temperature gradient in the silicon sample holder? Our calculations indicate that with the sample holder initially at 300 K and radiated by a blackbody at 873 K, the maximum radial temperature gradient is approximately 0.2 K/cm. Of course this temperature gradient necessarily decreases as the temperature of the sample holder approaches that of the blackbody radiator. The third question is by how much is the thermocouple junction temperature lowered due to heat conduction loses down the Pt wires? For the case in which our thermocouple is suspended in vacuum, our calculations indicate that the steady-state junction temperature is lowered by approximately 1 K at 873 K due to heat conduction loses down the Pt wires. In order

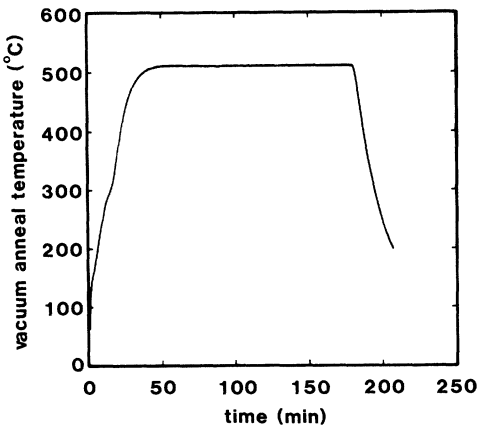

FIG. 2. Typical time-temperature profile obtained during a vacuum thermal anneal.

to minimize this error, the thermocouple junction is placed in thermal contact with the sample holder by placing the tip of the thermal couple in a small hole. Thermal contact is made by packing the hole with Pt wire. In view of these considerations the silicon sample temperature is taken to be the same as that measured by the Pt thermocouple.

In the case of the vacuum anneals, it is impossible to impose a rectangular time-temperature profile. A typical time-temperature annealing profile is shown in Fig. 2. To avoid any shortcomings or undue approximations from this limitation, we record the sample temperature as a function of time; the time and temperature are measured every second, digitized, and stored for subsequent analysis (Sec. III). Thus, the measured time-temperature profile is mathematically convolved into our kinetic analysis.

E. Thermochemical effects

Various chemical effects involving hydrogen and P_b centers as observed by EPR are summarized in Fig. 3. After dry thermal oxidation of (111) silicon at 850 °C,[18] we observe the P_b resonance as illustrated in Fig. 3(a). If in addition to thermal oxidation, the samples are subsequently reheated and annealed in vacuum for 1 hour at 850 °C, the P_b resonance appears to be unchanged [Fig. 3(b)]. P_b centers appear to be stable under thermal annealing for temperatures up to at least 850 °C. On the other hand, if after oxidation the samples are annealed in H_2 at only 300 °C for 90 min, then the P_b center is just barely detectable [Fig. 3(c)]. In this case the loss of signal is attributed to the passivation of P_b centers which renders them diamagnetic. We observe that the effects of passivation can be reversed as evidenced by the reappearance of the P_b resonance in Fig. 3(d) by annealing the samples in vacuum at approximately 675 °C; this latter effect is the focus of attention in this paper.

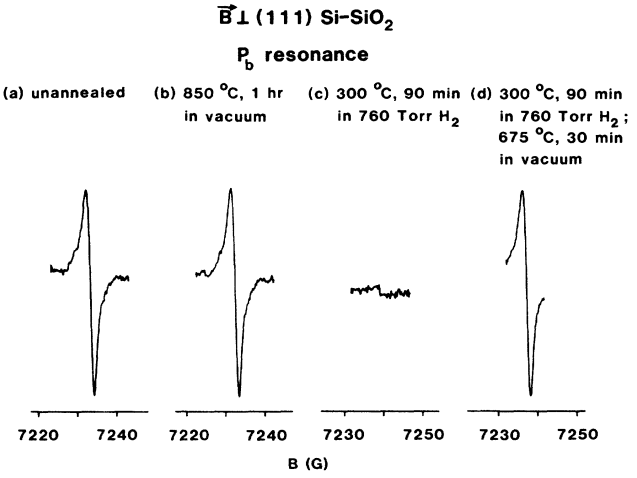

FIG. 3. Thermochemical effects on the P_b resonance at $g=2.0016$ as indicated by changes in the spectral intensity. (Changes in field position are due only to changes in the resonant cavity frequency and are not significant). The vertical sensitivity is the same for all four spectra. (a) P_b spectrum as observed after dry thermal oxidation of (111) silicon substrates at 850 °C (Ref. 18). (b) Subsequent *in situ* vacuum thermal annealing at temperatures up to 850 °C have no apparent affect on the P_b centers. (c) P_b centers are passivated by annealing in H_2 at 300 °C. (d) All of the P_b centers are recovered upon *in situ* vacuum annealing in this case at 675 °C.

III. EXPERIMENTAL RESULTS AND ANALYSIS

The results of the analysis presented here are consistent with the assumption that the recovery in the P_b signal follows first-order kinetics for which the rate equation is given by the expression

$$\frac{d[P_b]}{dt}=k_d(N_0-[P_b]) , \tag{4}$$

and the rate constant is given by the Arrhenius expression

$$k_d=k_{d0}\exp(-E_d/kT) . \tag{5}$$

Thus, the calculated concentration of P_b centers, $[P_b]_{\text{calc}}$ reappearing after a vacuum thermal annealing is given by the expression

$$[P_b]_{\text{calc}}=N_0\left[1-\exp\left[-k_{d0}\int_{T\text{ profile}}\exp[-E_d/kT(t)]dt\right]\right] , \tag{6}$$

where N_0 is the initial concentration of HP_b centers, or the maximum concentration of recoverable P_b centers as measured by EPR. Notice that in this solution to the rate equation the time-temperature profile, which is measured experimentally and denoted by the function $T(t)$, is folded into the expression for $[P_b]_{\text{calc}}$.

In our least-squares-fit analysis to determine E_d and k_{d0}, the calculated values given by Eq. (6) were least-squares fitted to the experimental values, $[P_b]_{\text{expt}}$, as a function of E_d and k_{d0}. In order to establish the validity of the kinetic model, it is necessary to acquire data over as wide a range of temperatures and $[P_b]/N_0$ ratios as possible. A range of temperatures is needed in order to determine E_d and k_{d0}; a range of $[P_b]/N_0$ ratios is needed in order to verify the time dependence implied in the rate equation. Our vacuum thermal anneals ranged from 500 to 595 °C, and the ratio in our measured values of $[P_b]/N_0$ ranged from 0.2 to nearly 1.0. Although it would be highly desirable to test our kinetic model for ratios of $[P_b]/N_0$ extending over several decades, this has

not been possible due to the limitations in the signal to noise of the P_b resonance.

The results of a least-squares fit with respect to E_d and k_{d0} pertaining to the recovery of P_b centers after hydrogen passivation are illustrated in Fig. 4 where $[P_b]_{\text{expt}}$ is plotted versus $[P_b]_{\text{calc}}$. For these data, which involve passivation with H_2, the results of our analysis indicate that this first-order kinetic process proceeds with an activation energy E_d of 2.56 eV±0.06 eV and a preexponential factor k_{d0}, of approximately 1.2×10^{12} sec^{-1}. The standard deviation in $[P_b]_{\text{expt}}$ from $[P_b]_{\text{calc}}$ is 4.4 which is to be compared with N_0 having a measured, relative value of 92.

A similar plot of $[P_b]_{\text{expt}}$ versus $[P_b]_{\text{calc}}$ for our deuterium data is presented in Fig. 5. In this case the temperature of our vacuum anneals was restricted to approximately 510 °C. A least-squares fit of these data, keeping the activation energy constant and equal to 2.56 eV, gave a preexponential factor k_{d0}, of 9.8×10^{11} sec^{-1} with a standard deviation in $[P_b]_{\text{expt}}$ from $[P_b]_{\text{calc}}$ of 3.7. The significance of the deuterium data in comparison with the hydrogen data is discussed in Sec. IV.

The correctness in the time dependence implied by the rate equation [Eq. (4)] is demonstrated in Fig. 6 where we have plotted $\log_{10}(1-[P_b]_{\text{expt}}/N_0)$ versus time t for fixed temperature (approximately 510 °C). In order to also show as distinctly as possible the effects of hydrogen mass on the rate of the dissociation process, we also show in Fig. 6 how the decay rate is affected by the hydrogen isotope used in the passivation process. The solid line in Fig. 6 representing the hydrogen data was calculated using the kinetic parameters deduced from the data in Fig. 4, and the dashed line representing the deuterium data was calculated using the kinetic parameters deduced from the data in Fig. 5. A relatively low temperature was selected so that the time-temperature profile was essentially square to a first approximation, and the experimental data could be plotted as a function of time for essentially constant temperature.

In order to show the quality of the least-squares fit as a function of temperature, which is essentially an indication of the adequacy of the Arrhenius expression for the temperature dependence in our model, the values for $([P_b]_{\text{expt}}-[P_b]_{\text{calc}})/N_0$ pertaining to our hydrogen data in Fig. 4 are plotted as a function of temperature in Fig. 7.

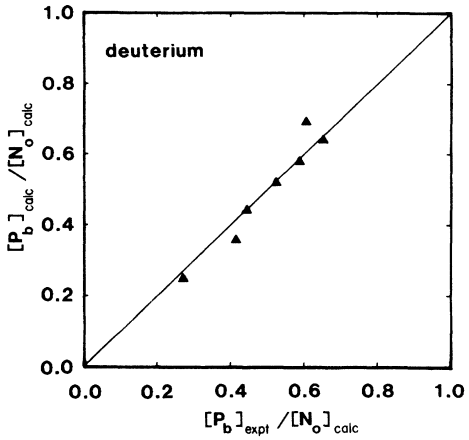

FIG. 5. Plot of the fraction of P_b centers measured experimentally after deuterium passivation and vacuum thermal annealing at 510.8 °C vs the calculated fraction of P_b centers as determined by a least-squares fit with respect to only the preexponential factor k_{d0}; the value for E_d was constant and equal to that deduced from the data in Fig. 4.

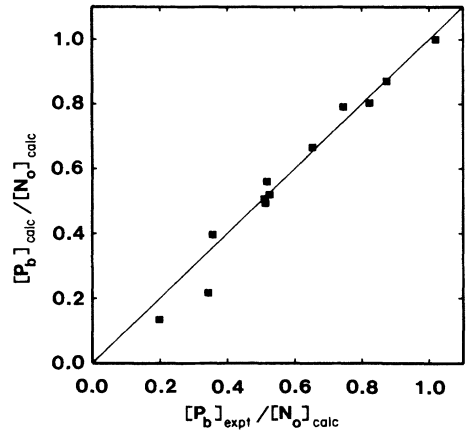

FIG. 4. Plot of the fraction of P_b centers measured experimentally after hydrogen passivation and vacuum thermal annealing vs the calculated fraction of P_b centers as determined by a least-squares fit with respect to the activation energy E_d and the preexponential factor k_{d0}. The vacuum anneal temperatures ranged from 500 to 595 °C. The solid line represents the ideal relationship.

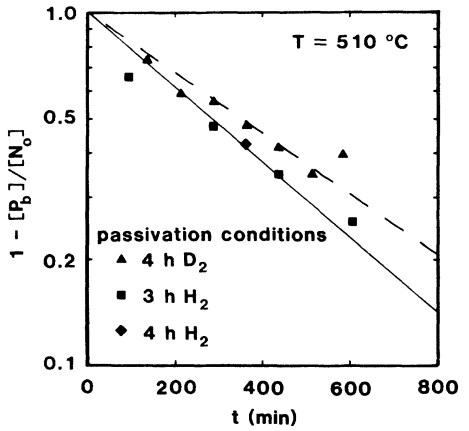

FIG. 6. Semilogarithmic plot of the fraction of HP_b centers $(=1-[P_b]_{\text{expt}}/N_0)$ as a function of annealing times at 510.8 °C assuming a rectangular time-temperature profile. The solid line corresponds to the calculated fraction of HP_b centers; the dashed line corresponds to the calculated fraction of DP_b centers.

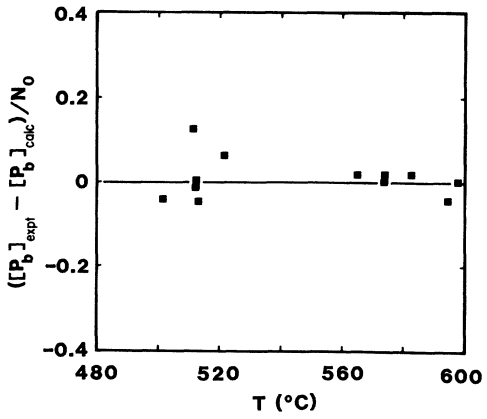

FIG. 7. Plot showing the distribution of experimental points as a function of the peak annealing temperature.

The sensitivity of the hydrogen preexponential factor k_{d0}, to small changes in the activation energy E_d, is shown in Fig. 8. This plot is based on a least-squares fit of the hydrogen data in Fig. 4 as a function E_d for fixed values of k_{d0} indicated in Fig. 8. The optimum values for E_d and k_{d0} cited above are indicated by the square data point in Fig. 8.

The standard deviation in $[P_b]_{expt}$ from $[P_b]_{calc}$ as a function of k_{d0} based on a least-squares fit of the hydrogen data in Fig. 4 with respect to E_d for fixed k_{d0} is illustrated in Fig. 9. These data indicate that there is one distinct solution pertaining to the fit of the experimental data to the kinetic equations [Eqs. (4) and (5)]. The square data point corresponds to the optimum value for k_{d0} cited in this paper.

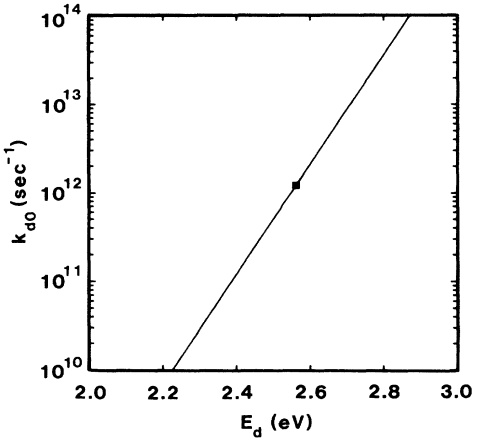

FIG. 8. Plot of k_{d0} as a function of the activation energy E_d, based on a least-squares fit of the data set in Fig. 4 for fixed values of k_{d0}. This plot shows the sensitivity in the value of k_{d0} for small changes in the activation energy. The square data point indicates the optimum values for E_d and k_{d0}.

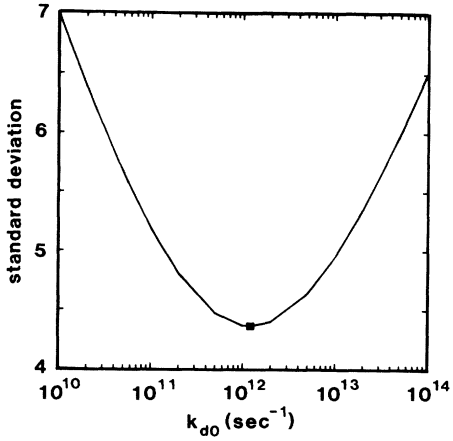

FIG. 9. Plot of the standard deviation in $[P_b]_{expt}$ from $[P_b]_{calc}$ resulting from a least-squares fit of the data set in Fig. 4 as function of E_d for fixed values of k_{d0}. N_0 has a relative value of 92. The data point at the minimum corresponds to the optimum values for E_d and k_{d0} cited in this paper.

IV. CHEMICAL PROCESSES

We consider two chemical processes with first-order kinetics that might conceivably be consistent with the recovery of the P_b signal upon annealing. We will show that the HP_b dissociation model is consistent with all the known experimental facts, whereas the oxygen diffusion model is inconsistent with known facts.

A. HP_b dissociation model

Since the annealing is done in vacuum, the most obvious chemical process is simply the dissociation of the HP_b center according to the reaction

$$HP_b \rightarrow P_b + H \ . \tag{7}$$

The rate of dissociation in this case should be sensitive to the isotopic mass of the hydrogen. To a first approximation, the rate constant is given by the expression

$$k_d = \nu e^{\Delta S/k} e^{-\Delta H/kT} \ , \tag{8}$$

where ν is an attempt frequency, ΔS is the change in entropy, which for silicon might typically be several Boltzmann factors, and ΔH is the change in enthalpy. The important point is that in this model the attempt frequency arises physically from vibrations involving the hydrogen, stretching and/or wagging, whose resonant frequencies would be affected by the mass of the hydrogen isotope. In the harmonic-oscillator approximation, vibrational frequencies are inversely proportional to the square root of the vibrating mass. Also, the entropy factor is expected to be a function of the vibrational frequencies.[19]

In Fig. 6, $\log_{10}(1-[P_b]/N_0)$ is plotted versus the annealing time in vacuum at constant temperature for samples previously passivated with H_2 (square data points) or D_2 (triangular data points). These data show that there is

a significant difference depending upon the hydrogen isotope. The analysis of our experimental data in Sec. III indicates that the preexponential factor $[k(\mathrm{H})]_{d0}$ for the hydrogen data is 1.2×10^{12} sec^{-1} as compared to a value for $[k(\mathrm{D})]_{d0}$ of 0.98×10^{12} sec^{-1}. Thus, the experimental value for the ratio $[k(\mathrm{D})]_{d0}/[k(\mathrm{H})]_{d0}$ is 0.82. The change in the frequency factor in Eq. (8) is expected to yield $\nu(\mathrm{D})/\nu(\mathrm{H})$ equal to 0.71 in the harmonic-oscillator approximation. Thus, the magnitude of the observed change in the preexponential factor k_{d0}, due to hydrogen isotopic effects is reasonable, and the effect corroborates the $\mathrm{H}P_b$ dissociation model.

B. Oxygen interstitial diffusion model

This model suggests itself because the activation energy for the diffusion of bond-centered interstitial oxygen in silicon is 2.54 eV (Refs. 20 and 21) and is very nearly equal to the dissociation energy (2.56±0.06 eV) we have determined for the process involving the reappearance of the P_b center. This model presumes that under vacuum annealing the rate-limiting process is the diffusion of interstitial oxygen in the crystalline silicon from one bond-centered interstitial site to another. We postulate that if an interstitial oxygen atom happens to occupy a site immediately adjacent to the defect silicon atom in the $\mathrm{H}P_b$ center (site "*R*" in Fig. 10), then it spontaneously interacts with the $\mathrm{H}P_b$ center to form the P_b center devoid of any neighboring hydrogen as evidenced by the lack of hydrogen hyperfine spectra. The inference is that the OH radical escapes leaving the P_b center.

The rate-limiting process in this model is the diffusion of the isolated interstitial oxygen. No experimental evidence has been found indicating that hydrogen is a part of the oxygen interstitial or involved in its diffusion.[20,22] Thus, the rate-limiting step involving the diffusion of interstitial oxygen is expected to be independent of hydrogen isotope effects. This clearly contradicts the experimental results shown in Fig. 6 and under the known circumstances negates the oxygen interstitial diffusion model.

It is, nevertheless, important to check this conclusion from other viewpoints. Let us consider the kinetics of this model. Infrared measurements of the float-zone silicon substrate material used in our experiment indicate an oxygen concentration in the as-received samples of approximately 3.5×10^{15} interstitial oxygen/cm^3.[23] Since our samples were oxidized at 750° for 31 h, we estimate that the near-surface concentration of oxygen is approximately 5×10^{16} interstitial oxygen/cm^3.[24] The rate at which $\mathrm{H}P_b$ centers are reduced by diffusing interstitial oxygen atoms in this model is given by the expression

$$\frac{d[\mathrm{H}P_b]}{dt}=-J\left[\frac{[\mathrm{O}_i]}{2\rho}\right]^{(\frac{6}{5}+\frac{3}{6})}[\mathrm{H}P_b]\ , \tag{9}$$

where $[\mathrm{O}_i]$ is the equilibrium concentration of interstitial oxygen and ρ is the concentration of crystalline silicon atoms/cm^3. The parameter J is the oxygen interstitial jump rate as deduced from infrared stress-induced dichroism measurements[20] and is given by the expression

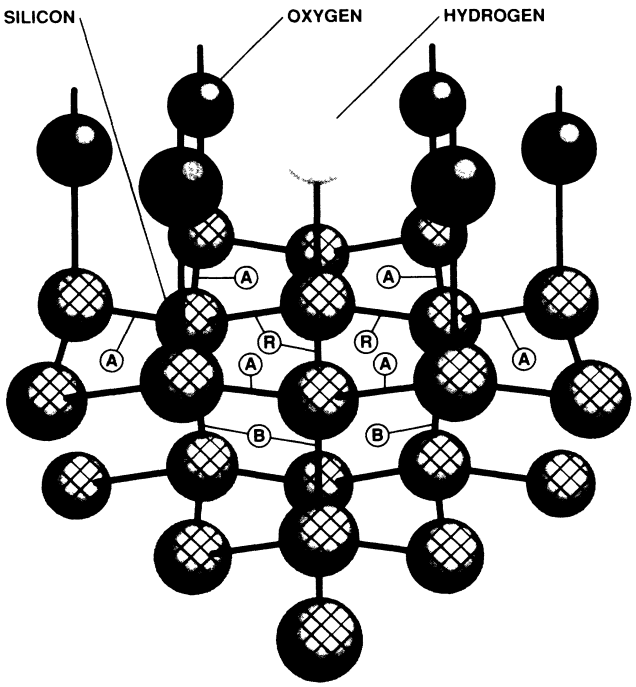

FIG. 10. Ball-and-stick model of the crystalline silicon environment around the $\mathrm{H}P_b$ center at the (111) Si-SiO_2 interface. Only the first layer of oxygen atoms of the thermal oxide is shown. The three first nearest-neighbor Si-Si bond-centered interstitial sites adjacent to the Si—H bond are denoted as "*R*." There are two distinct sets of bond-centered interstitial sites, denoted as "*A*" and "*B*," from which the oxygen interstitial can diffuse in jumping to the "*R*" sites. Interstitial oxygen atoms in the "*A*" sites are considered to have five jump options, one of which is the "*R*" site. Interstitial oxygen atoms in the "*B*" sites have six jump options, one of which is the "*R*" site and two the "*A*" sites.

$$J=J_0\exp(-E_{\mathrm{diff}}/kT)\ , \tag{10}$$

where E_{diff} is equal to 2.561±0.005 eV and J_0 is equal to 5×10^{15} sec^{-1}.[20] The first term on the right side of Eq. (9), namely $\frac{6}{5}$, indicates the probability that an oxygen interstitial occupying an "*A*" site jumps to a reaction site "*R*" in Fig. 10. If the oxygen atom jumps to the reaction site "*R*" in Fig. 10, then the chemical reaction resulting in the removal of the H atom from the P_b center proceeds spontaneously. The second term on the right-hand side in Eq. (9), namely $\frac{3}{6}$, indicates the probability that an oxygen interstitial in a "*B*" site jumps to an "*R*" site in Fig. 10. The form of Eqs. (9) and (10) indicates that the activation energy for the diffusion of the oxygen interstitial corresponds to the dissociation energy in Eq. (5) and the preexponential factor k_{d0}, in Eq. (5) corresponds to

$$k_{d0}=\frac{17[\mathrm{O}_i]}{20\rho}J_0\ . \tag{11}$$

The value of k_{d0} as predicted by Eq. (11) is 4.3×10^9 sec^{-1}. This value for k_{d0} is a factor of approximately 300 less than our experimental value of 1.2×10^{12} sec^{-1} and does not corroborate this model.

Finally, it does not appear energetically favorable for the oxygen atom to escape from the P_b center with the hydrogen atom as OH; it is energetically more favorable for the oxygen atom to remain bonded with or without the hydrogen to the silicon dangling bond of the P_b center in contradiction with experimental observation. This is based very simply on the relative bonding energies of H—O (4.44 eV), H—H (4.52 eV), O—Si (8.28 eV), and H—Si (3.09 eV).[25] For example, the difference in the binding energies of H—H and H—Si corresponds to 1.43 eV and is close to the experimentally measured value of 1.66 eV for the passivation reaction in Eq. (3) at the Si-SiO_2 interface.[15] These binding energies suggest that the Si—O binding will dominate over the O—H and Si—H binding configurations.

Thus, the oxygen interstitial model does not account for either the observed hydrogen isotopic effects, the oxygen-P_b reactivity rate, or the most energetically favorable chemical process and is therefore rejected.

V. ENERGY BARRIERS

It is important to note that the two chemical processes involving the passivation of the P_b center, Eq. (3), and the dissociation of the HP_b center, Eq. (7), are equivalent to the dissociation of the H_2 molecule,

$$H_2 \rightarrow H + H \ , \tag{12}$$

in the thermal oxide. Thus, the P_b center can be viewed as a catalyst facilitating the dissociation of the H_2 molecule. The dissociation energy of the H_2 molecule in vacuum is 4.52 eV.[25] Although the dissociation energy of the H_2 molecule in the interstices of the SiO_2 network might be smaller than in vacuum, this energy difference ε is expected to be small since, for example, the hyperfine splitting of interstitial atomic H^0 in SiO_2 is within 1% of the vacuum splitting. Also, SiO_2 is a rather tightly bound insulator with a band gap of approximately 9 eV. By comparing the energetics associated with the two possible chemical paths by which the H_2 molecule is in effect dissociated, the internal consistency of our models for the passivation of the P_b center and the dissociation of the HP_b center can be demonstrated. This line of reasoning with regard to the hydrogen kinetics of P_b centers has been noted previously.[15,16]

Let E_0, E_1, and E_2 be the difference in the total ground-state energies between the initial and the final constituents for each of the chemical reactions indicated by Eqs. (12), (3), and (7), respectively. According to the conservation of energy, this implies that for these chemical reactions $E_0 = E_1 + E_2$. However, during the course of a chemical reaction, the total energy may have to pass over a maximum energy as indicated by the dashed line in Fig. 11. The measured activation energy corresponds to E_α in Fig. 11 for a given chemical reaction. For the case involving the dissociation of the H_2 molecule in vacuum, it is important to realize that the energy barrier simply increases monotonically as illustrated schematically by the solid line in Fig. 11.[26] Furthermore, we suggest that the energy barrier for the dissociation of the H_2 molecule in the interstices of the SiO_2 is also monotonically increasing and nearly the same as that in vacuum for reasons mentioned above. Thus, the constraint on the activation energies for the two different chemical paths by which the H_2 molecule can be dissociated is

$$E_{H_2}^{vac} - \varepsilon = E_{H_2}^{SiO_2} \leq E_f + E_d \ , \tag{13}$$

where ε is expected to be small. Our experimental results indicate that $E_f + E_d$ is equal to 4.22 eV as compared to 4.52 eV for $E_{H_2}^{vac}$. The fact that $E_f + E_d$ is only 7% smaller than the dissociation energy of the H_2 molecule in vacuum suggests that the dissociation energy of the H_2 molecule in the interstices of the SiO_2, $E_{H_2}^{SiO_2}$, is approximately 4.22 eV according to Eq. (13). The self-consistency in the values for the activation energies in Eq. (13) also supports the chemical models that we have proposed for the passivation and dissociation processes.

Furthermore, in order to keep ε as small as possible in Eq. (13) and since there already is a 7% deficit, we suggest that the activation energies for the passivation and dissociation processes are equal or possibly only slightly greater than the difference in the total energy between the respective initial and final constituents as indicated schematically in Fig. 11. A montonically increasing energy barrier for the dissociation process appears reasonable since this two-body process is very similar quantum mechanically to the dissociation of the H_2 molecule; however, the nature of the energy barrier for the H_2 passivation process [Eq. (3)] is less obvious since this is primarily a three-body problem. If in fact there is a slight intermediate barrier (dotted line in Fig. 11) to either the passivation or dissociation processes, then this will necessitate a corresponding reduction in our estimate of the dissociation energy for the H_2 molecule in the oxide according to Eq. (13).

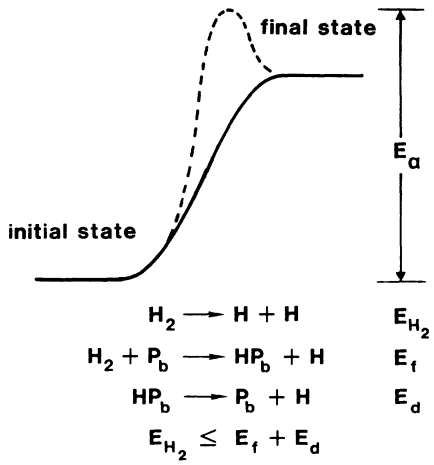

FIG. 11. Unified model for the hydrogen chemistry and kinetics of P_b centers at the (111) Si-SiO_2 interface. The measured values for E_f and E_d are (1.66±0.06) and (2.56±0.06) eV, respectively. The dissociation energy of the H_2 molecule in vacuum is 4.52 eV; our results suggest that the dissociation energy of the H_2 molecule in the thermal oxide is approximately 4.22 eV.

These energy considerations suggest that the reverse passivation reaction,

$$H + HP_b \rightarrow P_b + H_2 , \quad (14)$$

and the reverse dissociation reaction,

$$H + P_b \rightarrow HP_b , \quad (15)$$

are exothermic chemical reactions that might occur spontaneously, provided that atomic hydrogen is made available. The availability of atomic hydrogen is the controlling factor in the occurrence of these reverse reactions. Thus, the rate at which these reverse chemical reactions proceed is predicted to be either source limited, that is, limited by the rate at which atomic H is generated, or diffusion-limited, that is, limited by the rate at which H can reach the P_b center. Defect trapping of the atomic hydrogen may also be an important aspect of any actual problem.[15]

It has been demonstrated that ionizing radiation results in the release of atomic hydrogen within a typical thermal oxide; thus these exothermic reactions may well occur at relatively low temperatures in a radiation environment.[27,28] In the presence of atomic hydrogen the P_b center can be either passivated [Eq. (15)] or the HP_b center dissociated [Eq. (14)] as suggested by others.[8,28] In a radiation environment the competition between these chemical reactions might be a mechanism that introduces metastability in the relative number of P_b and HP_b centers. This metastability may be one of the reasons that account for the difficulty in understanding the effects of radiation on interface states.

VI. CONCLUSIONS

From this work emerges a unified model for the hydrogen chemistry and kinetics of (111) Si-SiO_2 interface defects known as P_b centers. The essence of this unified model is summarized in Fig. 11. As indicated in Fig. 11, P_b centers can be passivated with molecular hydrogen to form HP_b centers. The activation energy E_f, for this reaction is (1.66±0.06) eV.[12] Under vacuum thermal annealing the studies in this paper indicate that HP_b centers dissociate with an activation energy of (2.56±0.06) eV. The Arrhenius preexponential factor for hydrogen is approximately 1.2×10^{12} sec^{-1} and is smaller by a factor of 0.82 for DP_b dissociation.

The hydrogen molecule has an activation energy for dissociation of 4.52 eV in vacuum.[25] The dissociation energy for H_2 might be only slightly reduced in the thermal oxide due to weak interaction with the lattice; therefore it is expected to be *thermally* stable in the oxide up to at least 600 °C at which temperature chemical absorption commences.[29] However, the two-step process of passivation and dissociation is equivalent to the dissociation of the H_2 molecule and can occur below 600 °C. Because of the equivalence between these two chemical paths, there is a constraint between the activation energies for these chemical reactions as indicated in Fig. 11 [Eq. (13)]. This is a particularly strong constraint since it is well known that the energy barrier for the dissociation of the H_2 molecule is monotonically increasing as indicated schematically by the solid line in Fig. 11. This constraint indicates that the maximum total energy of the intermediate reaction configurations in both the passivation and the dissociation reactions is essentially bounded by the initial and final total energies. Although the shape of the energy barrier is not known, a monotonically increasing energy barrier for the passivation and dissociation processes such as illustrated in Fig. 11 is consistent with this constraint. If in fact the dissociation energy for the H_2 molecule in the thermal oxide is less, then allowance for (slight) intermediate barriers (dotted line in Fig. 11) in the dissociation-passivation processes may be necessary. These results are consistent with the idea that the dissociation energy of the H_2 molecule in the thermal oxide is approximately 4.22 eV.

The nature of the energy barriers as shown schematically in Fig. 11 indicates that the reverse reactions occur essentially spontaneously. Obviously, they can only occur in the presence of atomic hydrogen, which ordinarily is a scarce entity. The reverse passivation reaction [Eq. (14)] generates P_b centers that can be passivated by the reverse dissociation reaction [Eq. (15)] to form HP_b centers; hence these reverse reactions appear to be cyclic. Those factors affecting the dominance of either reaction over the other have not yet been determined; however, the work of Reed and Plummer[9] suggests that the reverse dissociation reaction [Eq. (15)] dominates over the reverse passivation reaction [Eq. (14)]. The complexities of radiation effects, which do generate atomic hydrogen[27] within the oxide, become self-evident. Under exposure to atomic hydrogen the rate of the reverse passivation-dissociation reactions is expected to be limited primarily by H-diffusion, H-source generation, and/or H-defect trapping.

ACKNOWLEDGMENTS

Technical assistance for this work was provided by Roger Shrouf. Discussions with S. M. Myers, P. M. Richards, H. J. Stein, and S. K. Estreicher concerning various facets of this work are gratefully acknowledged. This work was performed at Sandia National Laboratories and supported by the U.S. Department of Energy under Contract No. DE-AC04-76DP00789.

[1]Y. Nishi, Jpn. J. Appl. Phys. **10**, 52 (1971).

[2]E. H. Poindexter, E. R. Ahlstrom, and P. J. Caplan, in *The Physics of SiO_2 and its Interfaces*, edited by S. T. Pantelides (Pergamon, New York, 1978), p. 227.

[3]P. J. Caplan, E. H. Poindexter, B. E. Deal, and R. R. Razouk, J. Appl. Phys. **50**, 5847 (1979).

[4]K. L. Brower, Appl. Phys. Lett. **43**, 1111 (1983).

[5]For a recent review of Si-SiO_2 defect physics, see the 13 papers

in Semicond. Sci. Technol. **4**, 961–1126 (1989).

[6]P. M. Lenahan and P. V. Dressendorfer, Appl. Phys. **41**, 542 (1982); **44**, 96 (1984); J. Appl. Phys. **55**, 3495 (1984).

[7]E. H. Poindexter, G. J. Gerardi, M.-E. Rueckel, P. J. Caplan, N. M. Johnson, and D. K. Biegelsen, J. Appl. Phys. **56**, 2844 (1984).

[8]L. Do Thanh and P. Balk, J. Electrochem. Soc.: Solid-State Sci. Technol. **135**, 1797 (1988).

[9]M. L. Reed and J. D. Plummer, Appl. Phys. Lett. **51**, 514 (1987); J. Appl. Phys. **63**, 5776 (1988).

[10]B. J. Fishbein, J. T. Watt, and J. D. Plummer, J. Electrochem. Soc.: Solid-State Sci. Technol. **134**, 674 (1987).

[11]E. P. Burte and P. Matthies, IEEE Trans. Nucl. Sci. **NS-35**, 1113 (1988).

[12]K. L. Brower, Phys. Rev. B **38**, 9657 (1988); Appl. Phys. Lett. **53**, 508 (1988); in *The Physics and Chemistry of SiO_2 and the Si-SiO_2 Interface,* edited by C. R. Helms and B. E. Deal (Plenum, New York, 1988), p. 308.

[13]J. F. Shackelford, P. L. Studt, and R. M. Fulrath, J. Appl. Phys. **43**, 1619 (1972).

[14]J. E. Shelby, J. Appl. Phys. **48**, 3387 (1977).

[15]S. M. Myers and P. M. Richards, J. Appl. Phys. **67**, 4064 (1990).

[16]K. L. Brower and S. M. Myers, Appl. Phys. Lett. **57**, 162 (1990).

[17]K. L. Brower, Semicond. Sci. Technol. **4**, 970 (1989).

[18]The "new" silicon substrates used for the most part in this study were from a different manufacturer than the "old" silicon substrates used in Ref. 12. The "new" silicon substrates were more lossy in our microwave cavity after thermal oxidation at 850 °C. This problem was resolved by changing the oxidation temperature to 750 °C. Oxidation of the "old" silicon substrates at 750 °C showed no difference in kinetic behavior from the "new" samples. The data in Fig. 3 happened to have been taken earlier using "old" silicon substrates oxidized at 850 °C.

[19]See, for example, F. Seitz, *The Modern Theory of Solids* (McGraw-Hill, New York, 1940), p. 311.

[20]J. W. Corbett, R. S. McDonald, and G. D. Watkins, J. Phys. Chem. Solids **25**, 873 (1964).

[21]M. Stavola, J. R. Patel, L. C. Kimerling, and P. E. Freeland, Appl. Phys. Lett. **42**, 73 (1983).

[22]H. J. Hrostowski and B. J. Alder, J. Chem. Phys. **33**, 980 (1960).

[23]H. J. Stein (private communication).

[24]J. C. Mikkelsen, Jr., in *Oxygen, Carbon, Hydrogen and Nitrogen in Crystalline Silicon,* Vol. 59 of *Materials Research Society Symposium Proceedings,* edited by J. C. Mikkelsen, Jr., S. J. Pearton, J. W. Corbett, and S. J. Pennycook (MRS, Pittsburgh, 1986), p. 19.

[25]*CRC Handbook of Chemistry and Physics,* edited by R. C. Weast (CRC, Boca Raton, FL, 1980), p. F-225.

[26]See, for example, L. Pauling and E. B. Wilson, *Introduction to Quantum Mechanics* (McGraw-Hill, New York, 1935), Chap. 12.

[27]K. L. Brower, P. M. Lenahan, and P. V. Dressendorfer, Appl. Phys. Lett. **41**, 251 (1982).

[28]D. L. Griscom, J. Appl. Phys. **58**, 2524 (1985).

[29]J. F. Shackelford and J. S. Masaryk, J. Non-Cryst. Solids **21**, 55 (1976).

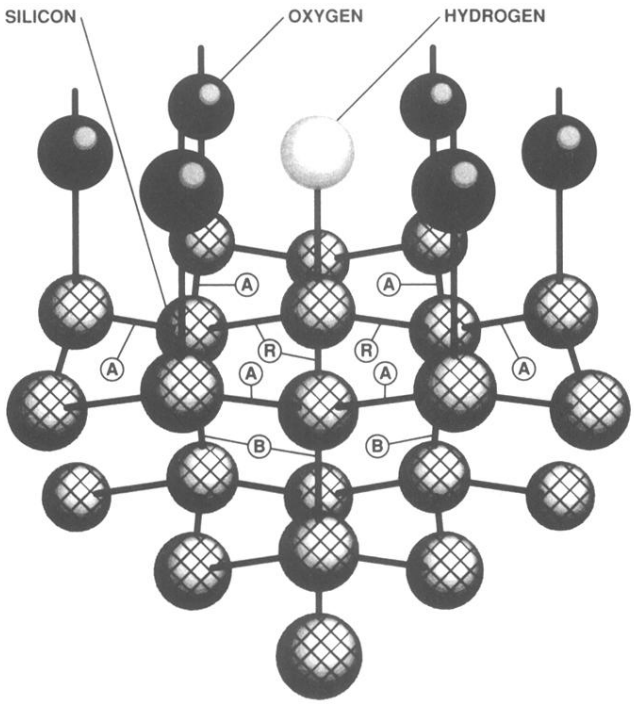

FIG. 10. Ball-and-stick model of the crystalline silicon environment around the HP_b center at the (111) Si-SiO_2 interface. Only the first layer of oxygen atoms of the thermal oxide is shown. The three first nearest-neighbor Si-Si bond-centered interstitial sites adjacent to the Si—H bond are denoted as "*R*." There are two distinct sets of bond-centered interstitial sites, denoted as "*A*" and "*B*," from which the oxygen interstitial can diffuse in jumping to the "*R*" sites. Interstitial oxygen atoms in the "*A*" sites are considered to have five jump options, one of which is the "*R*" site. Interstitial oxygen atoms in the "*B*" sites have six jump options, one of which is the "*R*" site and two the "*A*" sites.